Journal of Catalysis **203,** 292–306 (2001)
doi:10.1006/jcat.2001.3347, available online at http://www.idealibrary.com on IDEAL®

The Influence of Catalyst Restructuring on the Selective Hydrogenation of Acetylene to Ethylene

Yaming Jin,*,[1] Abhaya K. Datye,*,[2] Ed Rightor,† Robert Gulotty,† Wendy Waterman,† Michael Smith,† Michael Holbrook,§ Joe Maj,† and John Blackson†

*Center for Microengineered Materials and Department of Chemical and Nuclear Engineering, University of New Mexico, Albuquerque, New Mexico 87131; †Dow Chemical Company, Midland, Michigan 48667; ‡Dow Chemical Company, Freeport, Texas 77541; and §Dow Chemical Company, Plaquemine, Louisiana 70765

Received December 26, 2000; revised June 18, 2001; accepted June 28, 2001

Structural changes were induced in Pd and Pd–Ag catalysts by oxidation and reduction. The influence of oxidative restructuring on the selectivity for acetylene hydrogenation to ethylene was studied under conditions of industrial significance (acetylene conversion >99%). We found that oxidative restructuring of the Pd-only catalyst had no influence on hydrogenation selectivity; neither was any correlation found between selectivity and extent of β-Pd hydride formation. When Ag was added as a promoter, however, oxidation–reduction treatments had a major impact on selectivity. High-resolution transmission electron microscopy showed rough surfaces were created by oxidation of the catalyst which were coincident with poor selectivity. Annealing the catalyst at progressively higher temperatures in H_2 improved the selectivity to ethylene. Reduction in H_2 at 500°C also suppressed the formation of oligomeric hydrocarbon by-products during reaction. *In situ* **infrared study of CO adsorption showed that the addition of Ag to the Pd/silica results in an ensemble or geometric effect, increasing the proportion of linear CO relative to the bridged form. We infer that oxidation causes the Pd and Ag to segregate within the particle. High-temperature annealing in H_2 causes a migration of the promoter Ag so as to yield improved selectivity on these catalysts. The silica support surface also seems to provide a suitable environment to allow restructuring of the Pd–Ag crystallites to occur.**

Key Words: **selective hydrogenation of acetylene in ethylene; Pd–Ag bimetallic catalysts, characterization; Pd–Ag, oxidation and reduction of; IR spectroscopy of CO, on Pd–Ag.**

INTRODUCTION

Small amounts of acetylene (<3%) are present in ethylene derived from thermal pyrolysis or steam cracking. This acetylene is a poison for Ziegler–Natta polymerization catalysts and must be removed. Palladium-based catalysts have been used to selectively hydrogenate the acetylene impurity in the ethylene feedstock (1). The catalyst must meet two important criteria: selective hydrogenation of acetylene in the presence of a large amount of ethylene, and catalyst lifetime, which is governed by the deposition of oligomeric by-products (called green oil) on the catalyst. Hydrocarbon deposition fouls the catalyst, requiring regeneration by an oxidative treatment. The catalyst then needs to be reduced in H_2 before use, or simply activated *in situ*. Catalyst selectivity changes with time on stream, presumably due to changes in structure, as well as to the deposition of hydrocarbon species on the metal surface. Our work is directed at understanding the restructuring of the Pd catalysts as they are activated for reaction by reduction.

Selective hydrogenation of trace acetylene over Pd-based catalysts has been extensively studied. Some of the factors that have been suggested to alter catalyst selectivity include Pd particle size (2, 3), the presence of adatoms (4), and the formation of palladium hydride (2, 3). The interaction of these variables on the role of restructuring has not been explicitly investigated. Silver and other Group IB metals are commonly used additives for Pd catalysts used for selective hydrogenation of acetylene [e.g., (4–6)] and also of diolefins (7). Although widely used, the nature of the Pd–Ag bimetallic particles and the exact mechanism by which Ag modifies the selectivity of Pd catalysts are poorly understood.

In industrial operation, the acceptable acetylene content in the effluent should be lower than 10 ppm, and preferably less than 5 ppm (1), which corresponds to an acetylene conversion higher than 99%. The temperature where this is achieved is called the cleanup temperature. As reactor temperature is further increased, runaway ethylene hydrogenation can occur, which is manifested in an increase in the ethane/ethylene molar ratio. The temperature range between cleanup and runaway is of practical importance from an operational standpoint, since it is desirable to remove all of the acetylene from the ethylene stream without excessive loss of ethylene. Unfortunately, most academic research is

[1] Present address: Conoco Inc., Ponca City, OK 74602-1267.

[2] To whom correspondence should be addressed. E-mail: datye@unm.edu.

0021-9517/01 $35.00

performed at much lower conversions of acetylene (2, 3, 8–10). In a series reaction where acetylene → ethylene → ethane, selectivity is a function of overall conversion. Since acetylene is strongly adsorbed in preference to ethylene, the selectivity for acetylene conversion is high, until we approach complete conversion of acetylene. It is important to operate in this region to see clearly the differences between various catalysts.

In this study, we have evaluated the catalytic performance of Pd catalysts at high acetylene conversion, comparable to industrial conditions. We have worked under conditions that correspond to "front-end" hydrogenation, where the high hydrogen concentration makes it even more important to ensure selectivity and stability. This is in contrast to "tail-end" hydrogenation conditions, where hydrogen is fed in stoichiometric proportions and runaway is not important. We have studied the role of catalyst structure, role of Ag promoters, and influence of factors such as β-hydride formation. High-resolution transmission electron microscopy (HRTEM) was used to study the restructuring of Pd particles as they were used for this reaction. Temperature-programmed oxidation (TPO) provided unique insight into the extent of β-Pd hydride formation and carbon deposition in these catalysts. *In situ* IR spectroscopy was used to investigate the nature of Pd surface sites during reaction conditions.

EXPERIMENTAL

Sample Preparation

Four Pd catalysts were prepared by impregnation using 270-nm Stöber silica spheres as the support. Acetonitrile was used as the solvent for the $Pd(acac)_2$ precursor, while deionized water was the solvent for Pd nitrate and Ag nitrate. Pd_seq refers to the sequentially impregnated catalyst sample, for which Pd_1 was used as the precursor catalyst and was further impregnated with 0.25% Ag. Pd_coimp refers to the coimpregnated catalyst, in which the $Pd(NO_3)_2$ and $AgNO_3$ precursor salts were mixed and used for impregnation of the support. An additional monometallic Pd catalyst (Pd_2) was also prepared from the nitrate precursor to study the role of the metal precursor. After impregnation, the slurry was dried in an oven at 100°C for 24 h, then calcined at 600°C in air for 6 h. Table 1 summarizes chemical analysis results obtained from atomic absorption spectroscopy.

Reactivity Measurements

The selective hydrogenation reaction was performed in a fixed-bed quartz microreactor with 25 mg of catalyst loaded into the reactor and retained between quartz wool. The catalyst was studied in its as-prepared state and after several pretreatments. The pretreatments consisted of oxidation in 20% O_2 at 500°C, and in some cases this was followed by reduction in flowing H_2 at selected temperatures before introduction of the reaction mixture. A premixed gas consisting of 35% C_2H_4, 0.5% C_2H_2, 1000 ppm CO, and the balance N_2 was obtained from Scott Specialty Gases. The premixed gas (10 sccm) was mixed with 2 sccm of UHP H_2 to make the reaction mixture. For each reaction run, the reaction was started at 70°C. An on-line HP 5890 gas chromatograph was used to analyze the composition of the reaction effluent. The products were separated on a PLOT capillary column, CP-Al_2O_3/ Na_2SO_4 25 m × 0.25 mm × 4 μm, from Chrompack. Only hydrocarbon products are detected by the with the flame ionization detector, hence selectivity and conversion were based on analysis of the hydrocarbons alone.

TABLE 1

Chemical Analysis Results of Pd Catalysts

Catalyst	wt% Pd	wt% Ag	Precursor
Pd_1	0.45	—	$Pd(acac)_2$
Pd_2	0.47	—	$Pd(NO_3)_2$
Pd_seq	0.45	0.25	$Pd(acac)_2$ $AgNO_3$
Pd_coimp	0.46	0.27	$Pd(NO_3)_2$ $AgNO_3$

The selectivity of Pd catalysts was defined as:

$$\frac{C_2H_4 - C_2H_4(\text{feed})}{C_2H_2(\text{feed}) - C_2H_2} \times 100\%,$$

where C_2H_4 and C_2H_2 correspond to measured contents in the tail gas, and C_2H_4 (feed) and C_2H_2 (feed) refer to contents in the feed stream. To compare selectivities of different Pd catalysts, selectivity was plotted against ΔT, which is defined as ΔT = reaction temperature-cleanup temperature. The cleanup temperature is the temperature at which the effluent acetylene content reaches a low concentration, in our case 3 ppm, corresponding to >99% conversion of the incoming acetylene.

Catalyst Characterization

Pd particle size and morphology were characterized using transmission electron microscopy on a JEOL 2010 transmission electron microscope operated at 200 kev. The sample was supported on copper grids with holey carbon films by dipping the grid into the sample powder and shaking the excess. To follow the morphology of individual particles, the samples were supported on molybdenum grids, which were more stable during higher temperature reduction.

Temperature-programmed oxidation (TPO) was used to monitor the extent of hydride formation and to investigate

the nature of hydrocarbon species deposited during reaction. A mass spectrometer (Pffeifer-OmniStar 422) was used to monitor the gas-phase species formed during TPO.

Infrared measurements were taken in transmission mode using a Bio-Rad FTS-60A spectrometer. The catalyst was pressed at 1000 psi into 35-mg wafers of catalyst. A reaction flow cell (11) comprises the wafer sandwiched between NaCl windows (using graphite gaskets) in a stainless-steel mount. The reaction cell volume is ~0.5 ml; total flows of 16–20 ml/min were used. The gas compositions were 20% H_2 (balance He) for the reducing gas and purge gas and 1.3% C_2H_2/ 18% H_2 for the reaction gas. Samples were reduced from room temperature to 70 or 400°C with a ramp rate of 10°C /min and held for 1 h. CO adsorption measurements were taken at 50°C, after 5 min of purge gas flow. CO was removed from the surface by running the reaction mixture for 10 min. Running a mixture of C_2H_2 and H_2 in the absence of CO effectively removes the CO adsorbed on the Pd. This was the method used to generate a CO-free surface prior to the next CO adsorption experiment. Typical conversions of the samples reduced at 70°C were >98%, while those reduced at 400°C were 70–90% at 50°C.

RESULTS AND DISCUSSION

Effect of Pretreatment on Acetylene Hydrogenation Selectivity

Figure 1a shows the effect of reaction temperature on the selectivity of Pd_1 for acetylene hydrogenation in a large excess of ethylene. A selectivity of 100% would correspond to complete conversion of acetylene to ethylene, with no loss as ethane or other oligomeric products. When the selectivity is 0%, there is no net formation of ethylene; all the acetylene is hydrogenated to ethane or forms oligomers. Selectivities less than 0% correspond to a net loss of the reactant ethylene. With a series reaction of the type A → B → C, increasing conversion should lead to poorer selectivity for the intermediate product B (ethylene). This is evident in the data shown in Fig. 1 where selectivity decreases with increasing temperature. These results differ from recent work by Lambert and Gonzalez (12), who reported higher selectivity toward ethylene when the catalyst was operated at high temperatures (>300°C). These differences are related to the different reactor types and operating conditions used in these studies. Lambert and Gonzalez (12) used a membrane reactor where the contact time is short. Furthermore, at the high temperatures used in their work, the catalyst is probably extensively covered with carbonaceous species. Our work is performed using a packed bed and shorter times on stream, so we have not built up extensive deposits of hydrocarbon species on the catalyst. The selectivity behavior shown in Fig. 1 is comparable to other work in the literature (13), where increasing reaction temperature leads to decreased selectivity.

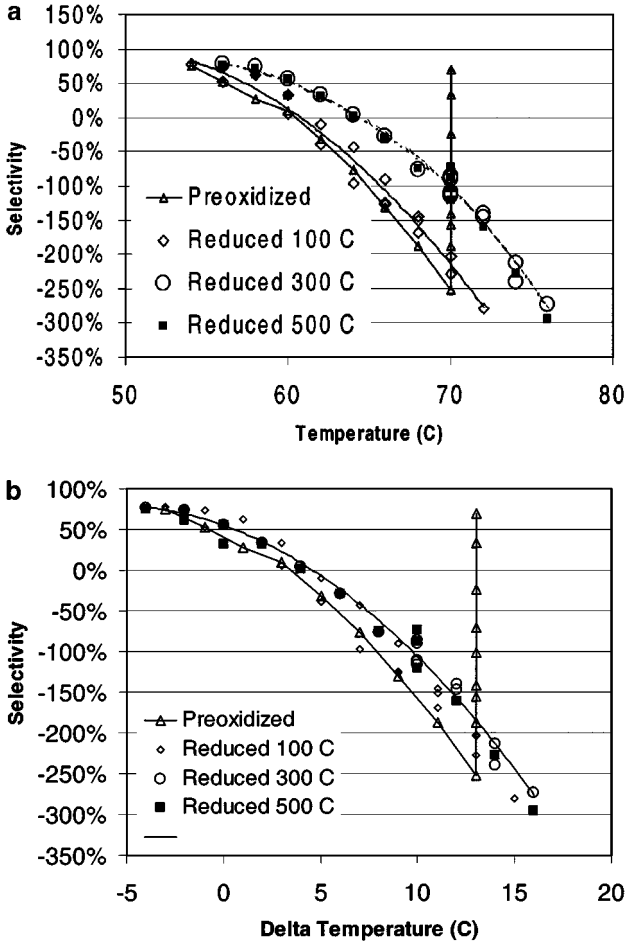

FIG. 1. (a) Selectivity of catalyst Pd_1 under different pretreatments: (1) no pretreatment (Preoxidized); (2) 20 ml/min H_2, 100°C for 1 h; (3) 20 ml/min H_2, 300°C for 1 h; (4) 20 ml/min H_2, 500°C for 1 h. (b) The same data plotted as a function of ΔT, the difference between reaction temperature and cleanup temperature.

Also shown in Fig. 1a is the effect of pretreatment. When preoxidized Pd is used, the catalyst shows an induction period as the catalyst is reduced *in situ* under reaction conditions into its metallic form. During the reduction, catalyst activity continues to increase with a corresponding drop in selectivity. This is shown in the series of points that lie on the vertical line. After being fully reduced, the catalyst exhibits its highest activity, but poorest selectivity. When the preoxidized catalyst is reduced in H_2 at increasingly higher temperatures, we see improved selectivity with a corresponding drop in activity. The selectivity versus temperature tends to fall on a single curve for any given pretreatment. The data suggest that as catalyst pretreatment temperature is increased, there is an improvement in selectivity. However, the differences seen here may be affected by overall conversion, which is also changing with pretreatment. To make this comparison meaningful, we need to compare catalysts

at similar activity. This can be accomplished by plotting selectivity as a function of ΔT, the difference between the reaction temperature and the cleanup temperature, as shown in Fig. 1b. The cleanup temperature is defined as the temperature at which acetylene content in the effluent reaches a predetermined value, in our case 3 ppm. Therefore, when $\Delta T = 0$, the cleanup temperature, we are comparing all catalysts at a similar conversion (99.3% conversion of acetylene).

Plotted in this way, we find that the selectivity of all of the prereduced catalysts appears to fall on one curve. We therefore conclude that the observed selectivity differences between different pretreatments in Fig. 1a can be traced to differing activities. The only significant difference is that between the preoxidized catalyst, with no pretreatment, and the catalysts that have been reduced in H_2. To understand the differences in the morphology of Pd particles, we examined these catalysts, as a function of pretreatment, using high-resolution transmission electron microscopy. The results are described in a later section.

Figure 2a shows the selectivity data for the sequentially impregnated catalyst (Pd_seq) under different pretreatments. In contrast to the monometallic Pd catalyst, the effects of pretreatment here are quite significant. Once again, the differences in selectivity are caused in part by the different activities of these catalysts. To account for the different activities, we replot selectivity as a function of ΔT, the difference between reaction temperature and cleanup temperature. Figure 2b shows that despite plotting against ΔT, there are clear differences in the selectivity-versus-temperature curves at differing pretreatment temperatures. Catalyst selectivity increases monotonically with pretreatment temperature in hydrogen, with the catalyst treated in H_2 at 500°C showing the highest selectivity. An important parameter in these catalysts is the difference between cleanup temperature and runaway temperature, the temperature at which ethylene selectivity starts to drop exponentially. The high-temperature H_2-treated catalyst shows the most desirable behavior in its loss of ethylene selectivity with increasing temperature. The catalyst with no pretreatment after oxidation shows the lowest selectivity and the narrowest operating window. It is interesting to note that the effects of oxidation–reduction treatment are reversible, the behavior of the 100°C pretreated sample is identical to that of the sample that was reoxidized and pretreated at 100°C in hydrogen.

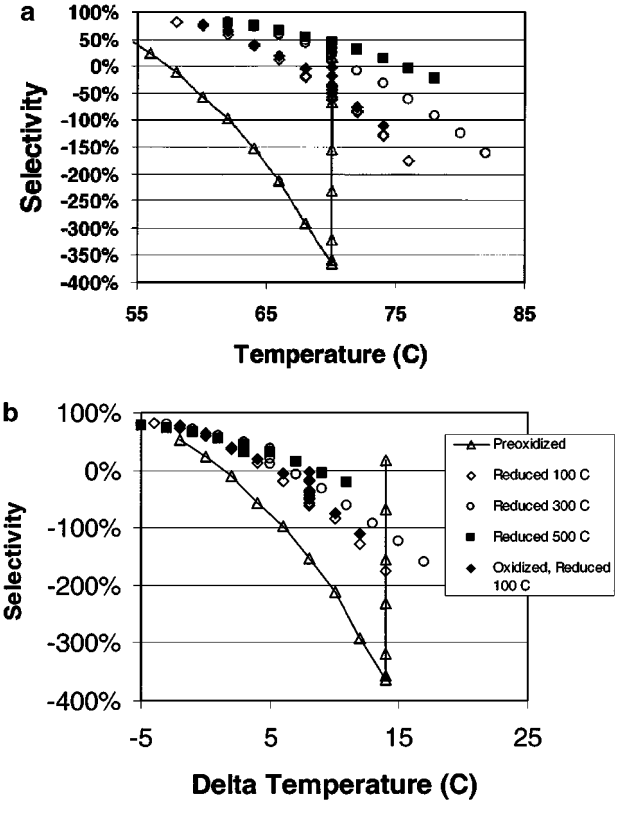

FIG. 2. (a) Selectivity of Pd_seq (the sequentially impregnated Pd, Ag catalyst) under different pretreatments: (1) no pretreatment; (2) 20 ml/min H_2, 100°C for 1 h; (3) after run 2, 20 ml/min H_2, at 300°C for 1 h; (4) after run 3, 20 ml/min H_2, at 500°C for 1 h; (5) after run 4, reoxidized and pretreated with 20 ml/min H_2, 100°C for 1 h. (b) The same data plotted as a function of ΔT.

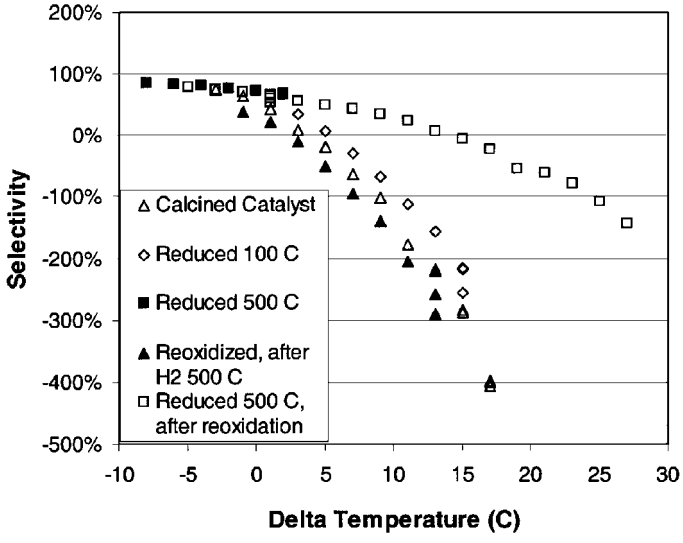

FIG. 3. Selectivity of Pd_coimp (the coimpregnated Pd, Ag catalyst) under different pretreatments: (1) no pretreatment: (2) 20 ml/min H_2, 500°C for 1 h; (3) after run 2, reoxidized and used without any further pretreatment; (4) reoxidized and reduced in H_2, 500°C for 1 h.

The selectivity behavior of the Pd, Ag coimpregnated catalyst (Pd_coimp) is shown in Fig. 3. Selectivity is now plotted against ΔT since in this manner we account for differences in catalyst activity. While the effect of H_2 treatment is similar to that on catalyst Pd_seq, the effects are even more dramatic. High-temperature treatments in H_2

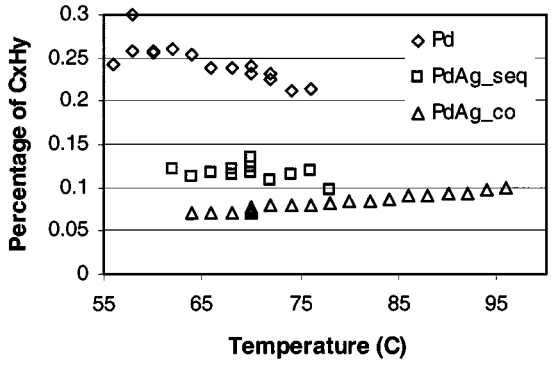

FIG. 4. By-product formation as a function of reaction temperature for the Pd catalysts.

yield higher selectivity and the least sensitivity to increases in temperature. Also significant is the absence of the induction period seen in all of the other catalysts. On this sample, when a preoxidized sample was introduced into the reaction mixture at 70°C, its reactivity reached a steady state very quickly.

An important operating characteristic of these catalysts is the presence of oligomeric by-products. These oligomers, known as green oil, tend to foul the catalyst and cause operational difficulties in industrial practice. A measure of by-product hydrocarbon formation is the additional peaks seen in GC analysis of the effluent. We have not attempted to identify the various species, but simply summed the areas of these peaks for the different catalysts. The total area of the oligomeric products is plotted as a percentage of the hydrocarbon products in Fig. 4. It can be seen that after H_2 treatment at 500°C, the Pd–Ag coimpregnated catalyst yields the smallest total peak area of hydrocarbon by-products. The GC analysis is confirmed by mass spectroscopic analysis of the oxidation products after reaction, as described below.

Nature of Hydrocarbon By-products Formed during Acetylene Hydrogenation

Temperature-programmed oxidation was performed in 10% O_2 in flowing helium, after the reaction was stopped and the catalyst cooled to room temperature and flushed in helium. The peaks corresponding to AMU 18 (H_2O) and 44 (CO_2) were monitored as a function of temperature during the temperature ramp. These TPO traces provide information on the nature of carbonaceous species present on the catalyst. They also provide an indication of the extent of β-hydride formation in the Pd metal crystallites, since the hydride decomposes readily and yields a water peak at low temperatures. It was surprising that the catalyst prepared from the $Pd(acac)_2$ precursor (Pd_1) showed no evidence of hydride formation. To confirm that this behavior was not a result of a kinetic limitation, the catalyst was left overnight in flowing H_2. There was no difference caused by overnight exposure to H_2, as we found that the acac-derived Pd catalyst was the only one that did not show any evidence of β-hydride formation. Since it has been speculated in the literature that the extent of hydride formation may influence selectivity for acetylene hydrogenation, we examined the TPO behavior of the two monometallic Pd catalysts. The results are shown in Figs. 5a and 5b. Both catalysts show evidence for the hydrocarbon species that accumulate on the catalyst during reaction (as H_2O and CO_2 is evolved simultaneously). No H_2O peak corresponding to the β-hydride is seen in the acac-derived catalyst. However, the lack of hydride formation does not appear to have any effect on the selectivity, since the selectivity behavior of the two monometallic catalysts is quite similar (not shown). The reason the Pd(acac) catalyst does not form the hydride phase could be a particle size effect. Particles smaller than 3 nm apparently do not form the β-hydride phase. TEM images revealed that small Pd metal particles were indeed seen on the acac-derived sample.

Since H_2 treatment had the most dramatic effect on the selectivity of the Pd–Ag coimpregnated catalyst, we studied the effect of pretreatment on the extent of hydrocarbon accumulation. Shown in Fig. 6 are the TPO data for this catalyst after 2 h reaction under similar conditions (60°C reaction temperature). The effect of the higher-temperature H_2 treatment is seen most dramatically in the sharp decrease in the hydrocarbon oxidation peak that occurs around 200°C. The nearly equal peak areas of the H_2O and CO_2 peaks suggest that the overall stoichiometry of the hydrocarbon species deposited on the catalyst is $C:H = 1:2$, which would be consistent with the products of oligomerization of acetylene.

HRTEM of Catalyst Restructuring Caused by Oxidation and Reduction

The dramatic effects caused by increasing reduction temperature in H_2 were investigated by performing *ex situ* examination of Pd catalysts. Samples were supported on holey carbon film on Mo grids, and subjected to H_2 treatment as well as to reaction conditions. The same region of the sample was examined before and after treatment. Figure 7a is a low-magnification image of the model Pd–Ag (Pd_coimp) catalyst in its as-prepared form after calcinations. The catalyst after exposure to reaction conditions at 70°C is shown in Fig. 7b, and the same region after treatment in H_2 at 500°C is shown in Fig. 7c. At this low magnification, we can see that the changes in particle shape are subtle, but there is indeed a definite accumulation of carbonaceous species on the catalyst surface after the high-temperature H_2 treatment. Figures 8a and 8b show similar sequences from the same catalyst but at higher magnification. It is evident that the Pd–Ag metal particles are rougher

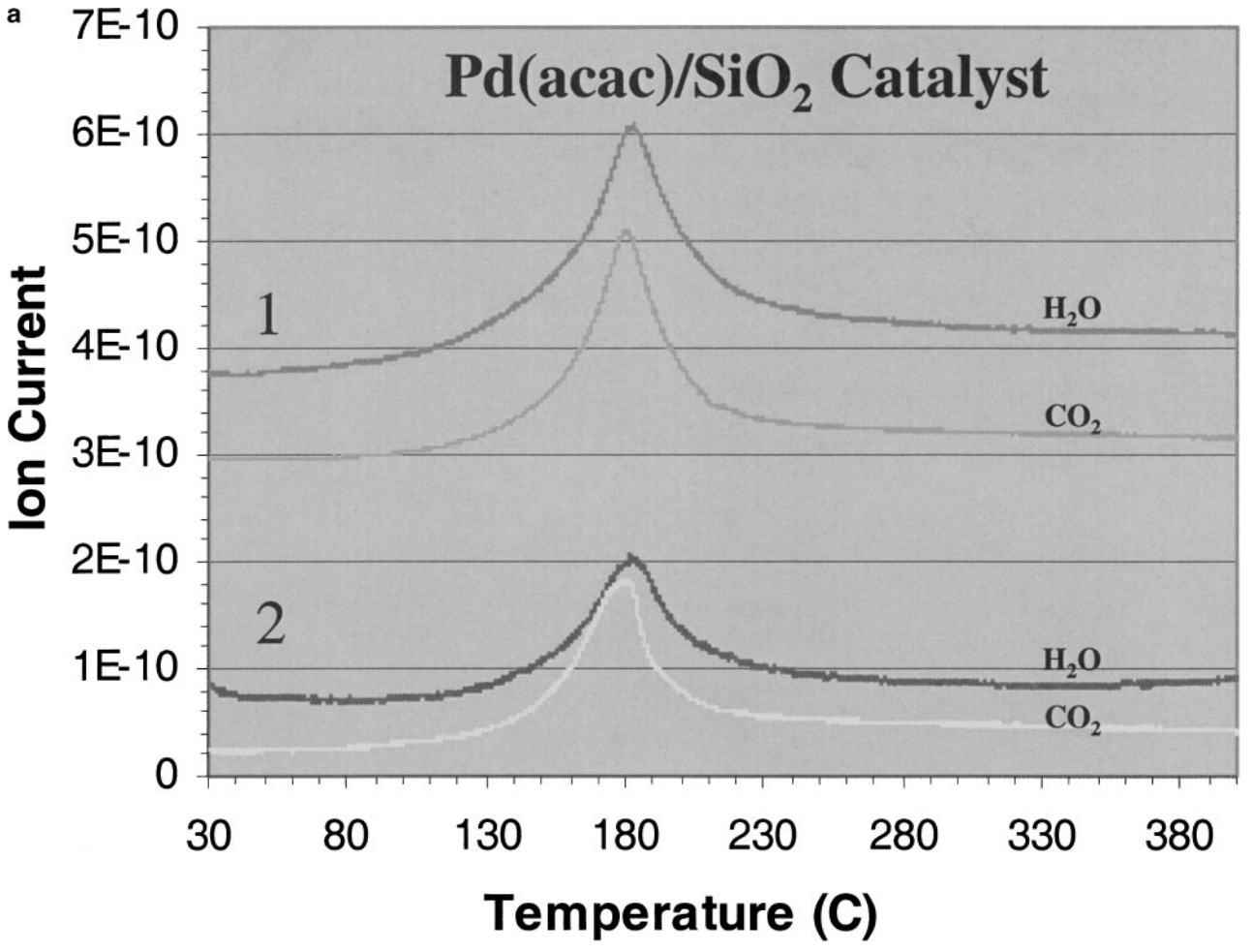

FIG. 5. Temperature-programmed oxidation after 2 h reaction: (a) $Pd(acac)_2$ catalyst (Pd_1), (b) $Pd(NO_3)_2$ catalyst (Pd_2). Curve 1 shows the data for a catalyst with no pretreatment; curve 2 shows the catalyst after 400°C treatment. The 400°C H_2 pretreatment does not affect the amount hydrocarbon species deposited on the Pd catalysts during reaction. Also, the $Pd(acac)_2$ catalyst shows no β-hydride formation under these conditions.

in their initial, calcined state. After reaction, the particles appear to shrink in size, which would be consistent with the loss of oxygen and higher density of the reduced, metallic form of the particle. H_2 reduction at 500°C causes the particles to become more spherical and these particles also show some surface facets consistent with the fcc structure of the metals involved. Surface facets are clearly seen only when the particle is oriented along a zone axis; hence not all images show these facets since the particles are randomly oriented.

The low-contrast haloes on the metal particles represent carbonaceous deposits that have formed on the metal surface. The H_2 treatment at 500°C was performed on the catalyst after it was used for reaction and examined by TEM. No intermediate oxidation step was performed. Hence, any carbonaceous species present on the catalyst surface could migrate on the surface and possibly get concentrated on the metal surface. The Pd–Ag catalyst used directly in its oxidized form has the lowest selectivity for ethylene formation and also shows the largest accumulation of hydrocarbon species as seen by subsequent TPO (see Fig. 6). It would be interesting to determine if these hydrocarbon species are present on the metal or on the support. Higher-magnification images of this catalyst are presented in Fig. 9 in the oxidized form and after reaction. Figure 9b does not provide any evidence for hydrocarbon deposits on the metal surface after reaction. We infer that the hydrocarbons are probably located on the support and they migrate to the metal surface during the H_2 treatment at 500°C. The oxide form of the catalyst shows lattice fringes of PdO. After reaction, it is clear that the particle has shrunk. After higher-temperature treatment in H_2, the particles adopt the fcc structure and we can clearly see lattice fringes corresponding to Pd metal (not shown).

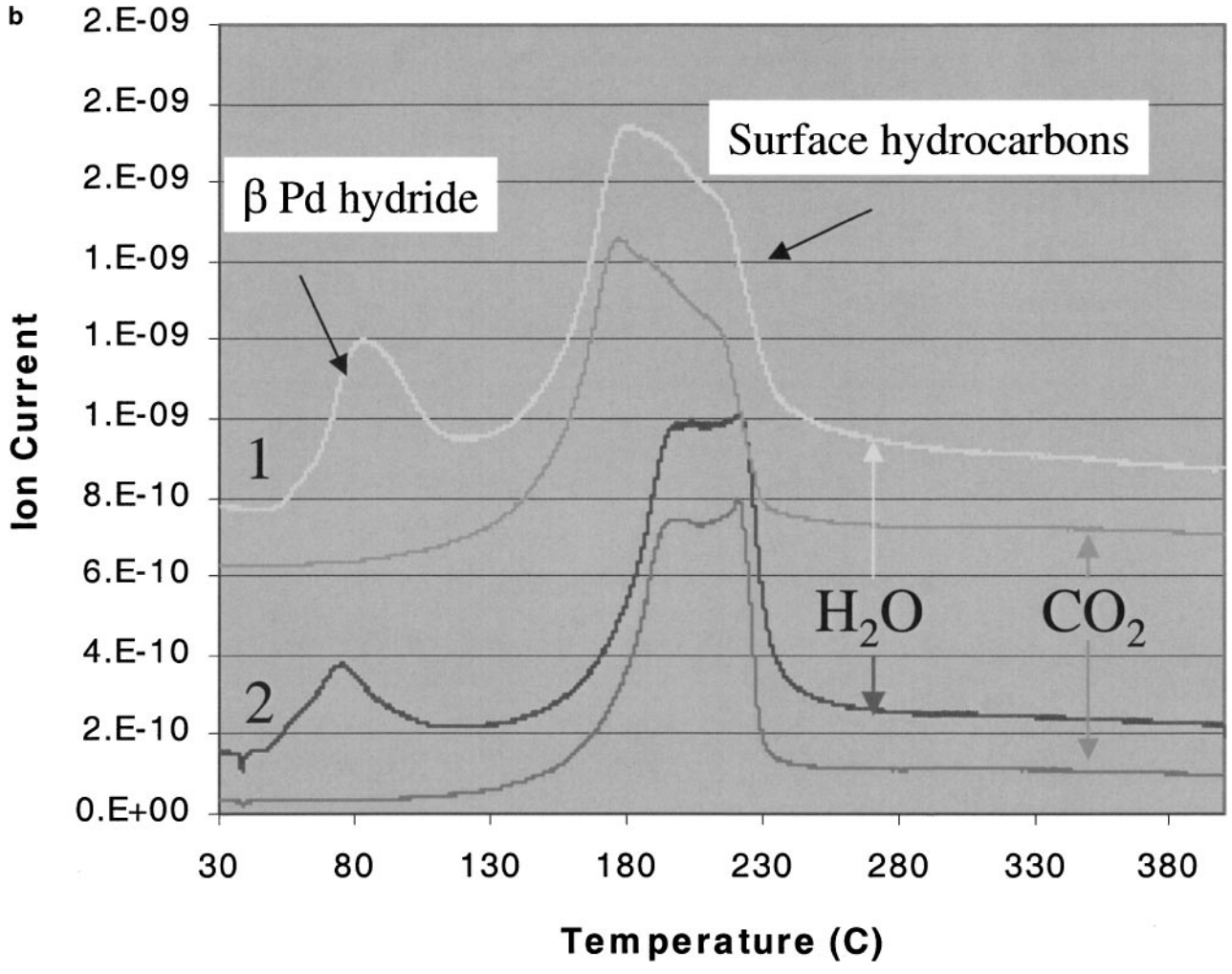

FIG. 5—*Continued*

In Situ Infrared Characterization of the Catalysts

The changes in Pd surface morphology were also studied using CO adsorption in a flow mode. The flow mode was used because a direct correlation could be made between the adsorbed CO and catalyst performance. Figure 10a shows the CO adsorption spectrum of a Pd/Silica catalyst reduced at 70°C. The sample was reduced by using 4 ml/min H_2 with 16 ml/min He starting at room temperature, ramping at 10°C/min to 70°C, and holding for 1 h. The sample was cooled to 50°C and preconditioned under a C_2H_2/H_2 reaction mixture for 10 min at 50°C. For CO adsorption, a flow of 0.73 ml/min 101 ppm CO/Ar was pulsed onto the sample in 1-s increments ($\sim$0.5 μmol CO/pulse, corresponding to 1/3 mol Pd of sample) for 10 pulses, followed by longer flow periods. After this, a higher concentration of CO was applied to the sample to obtain saturation coverage (190 Torr CO/He). The adsorbed CO from the first pulse gives primarily bridged CO sites with a peak maximum of 1893 cm^{-1}. The maximum absorbance shifts to higher frequencies with increasing coverage of CO. The shift in CO vibrational frequency reflects the heterogeneity of surface sites. With increasing coverage, dipole–dipole interactions among adsorbed CO cause a further shift in CO vibrational frequency. Linearly adsorbed CO (at 2050 cm^{-1}) starts to appear only at the highest coverage. Figure 10b shows the CO adsorption spectrum of the same catalyst, but after reduction in H_2 at 400°C. The absorbance is reduced by a factor of 10, suggesting sintering of metal particles resulting in a reduced metal surface area. Otherwise, the spectra in Fig. 10b are similar to those in Fig. 10a and show similar distributions of linear and bridged CO species after low- and high-temperature H_2 reduction.

The IR spectra of adsorbed CO for the Pd/Ag/Silica catalyst (Pd_coimp) after low-temperature reduction (70°C in flowing H_2) are shown in Fig. 11a. The reduction

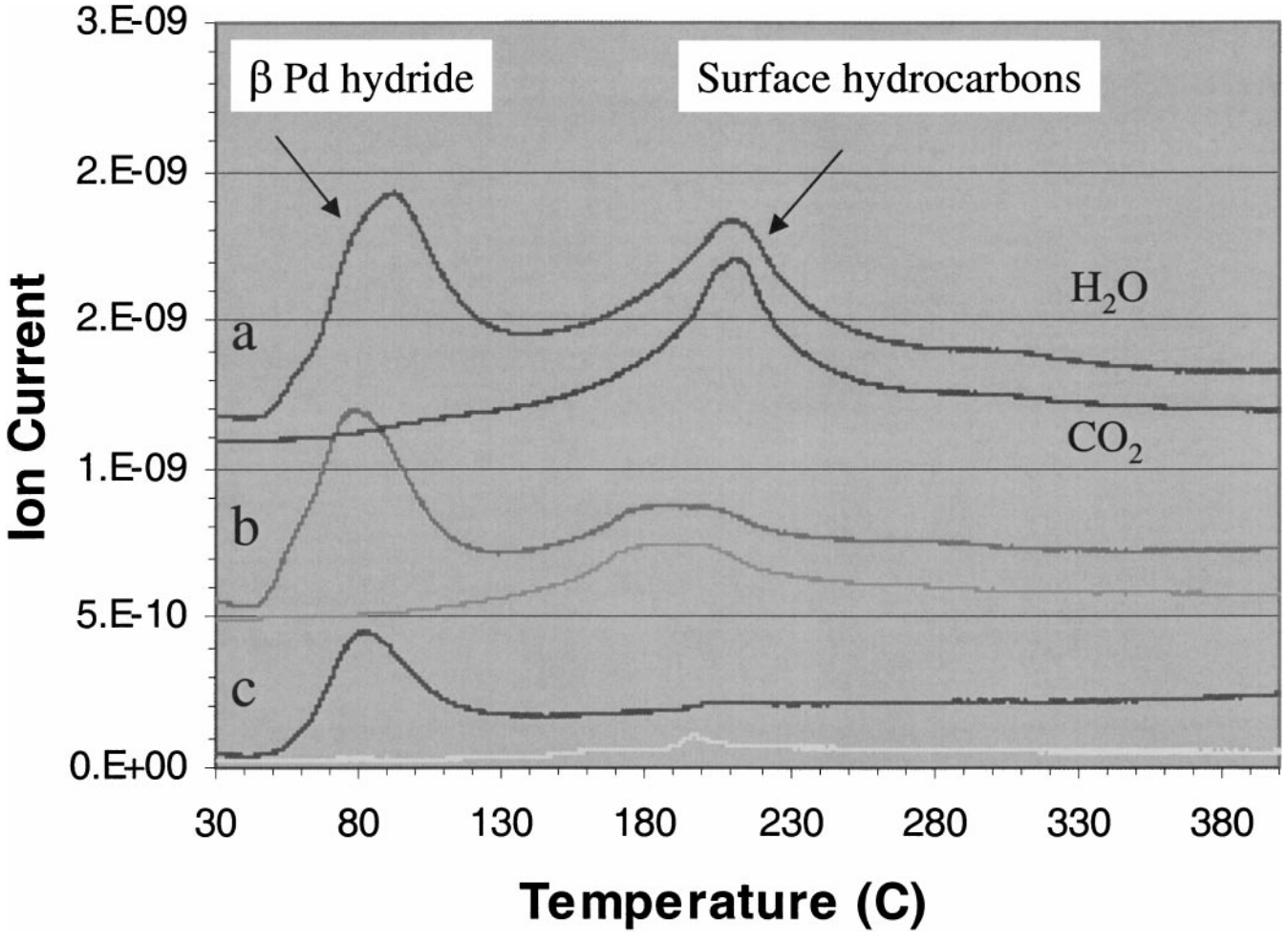

FIG. 6. Temperature-programmed oxidation after 2 h reaction on the Pd–Ag coimpregnated catalyst. Reduction in H_2 at 400°C has a major effect on the amount of carbonaceous species deposited on the catalyst, as seen from the areas of the H_2O and CO_2 peaks.

procedure and pretreatment in the reaction mixture were similar to those described for Fig. 10a. The behavior in the bridged region is similar to that of the Pd-only sample, but the fraction of CO in the form of linearly bonded CO is enhanced by the addition of Ag. In addition, the spectra appear broader in the bridged region, suggestive of larger heterogeneity in the Pd/Ag sample. A higher CO exposure is required to saturate the surface of the Pd/Ag sample than the silica-supported Pd-only sample. Figure 11b shows the CO adsorption spectra at 50°C for the Pd/Ag/silica catalyst after reduction at 400°C. The absorbance is reduced by a factor of 10 similar to that for the Pd-only catalyst, suggesting that sintering was occurring in both samples. However, there was a significant increase in linearly bonded CO for the Pd/Ag catalyst after the higher-temperature reduction. These data suggest that the effect of Ag on the Pd particles is a geometric dilution of surface Pd sites, in other words, an ensemble effect. No electronic effect was observed. This is not the case for Ag promotion of Pd particles on alumina (14), where both ensemble and electronic effects were reported.

Proposed Model for the Restructuring of Pd–Ag after Oxidation and Reduction Treatments

In this work, we have shown that high-temperature reduction in H_2 improves the performance of Pd–Ag catalysts for selective hydrogenation of acetylene to ethylene. While H_2 treatment at elevated temperature also causes changes in the morphology of monometallic Pd particles, the selectivity for acetylene hydrogenation on Pd is only marginally affected. The most dramatic effects are seen when Ag is present along with the Pd. These observations imply that the role of particle morphology by itself may not be significant; instead, the rearrangements in the Ag adatoms could be causing the observed changes in catalyst selectivity. The IR data suggest that the high-temperature reduction of Pd–Ag catalysts decreases the number of Pd nearest neighbors,

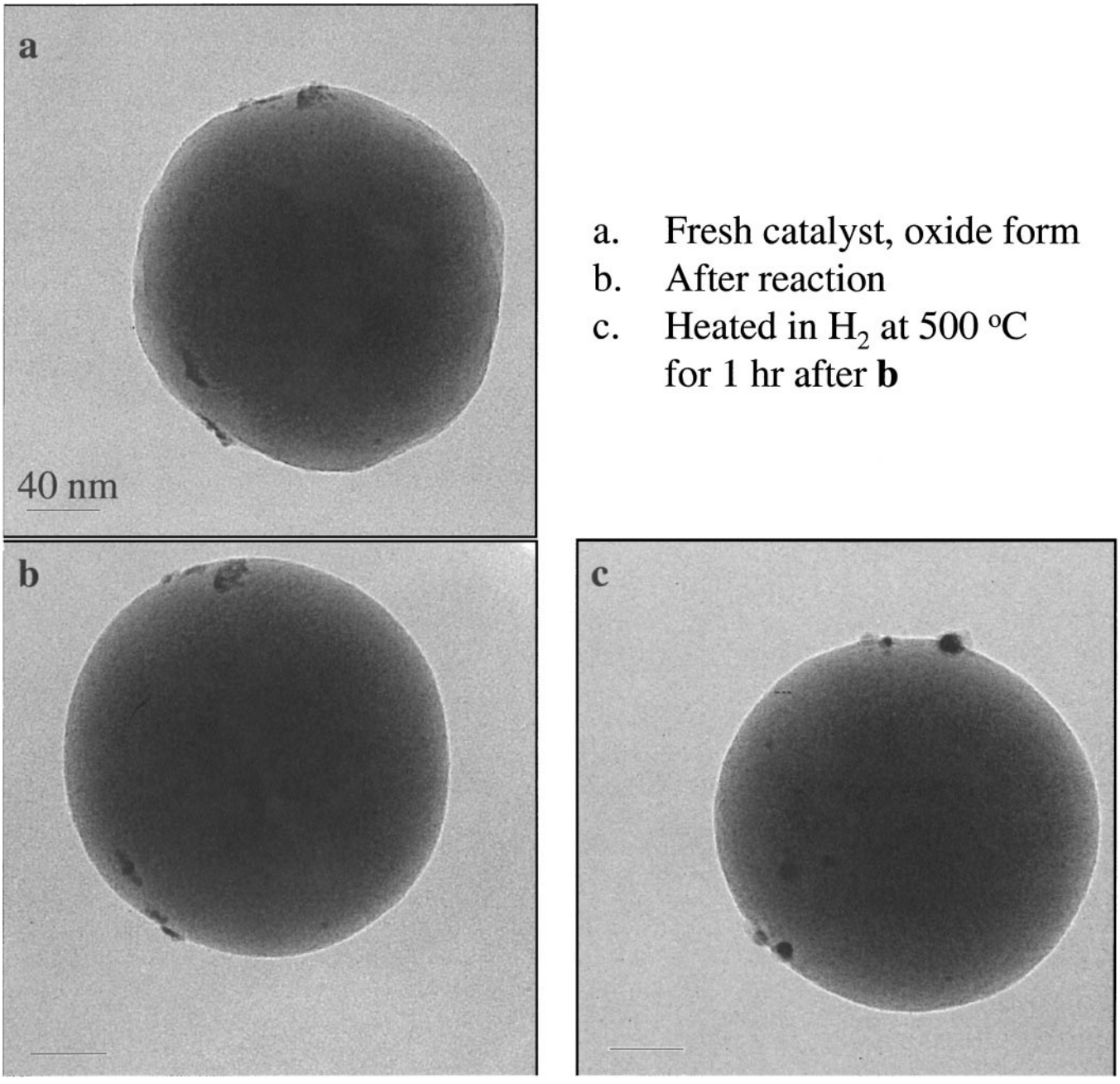

FIG. 7. Low-magnification TEM images of the model Pd–Ag coimpregnated catalyst as a function of treatment. The same area of the sample is being imaged. Heating in H_2 at 500°C makes the metal particles more spherical, but also seems to create lighter contrast haloes on the metal surface.

reducing the amount of bridge-bonded CO relative to linearly bonded CO.

Pd and Ag both crystallize on a fcc lattice and differ slightly in size; Ag has a radius of 144 pm while Pd is 137.6 pm. According to the literature (15), they should form a continuous series of solid solutions. In a study of electrochemically deposited powders, the authors (15) found that two types of solid solutions, Pd-rich with a maximum concentration of Ag of 8%, and Ag-rich, with a maximum Pd concentration of 15%. This work was on micrometer-sized Pd–Ag alloy powders which are of interest for making electrical contacts in microelectronic circuits (16) as well as in dental materials (17). Since the metal particles in hydrogenation catalysts are in the nanometer size range, much of the literature on Pd–Ag alloys is not directly relevant.

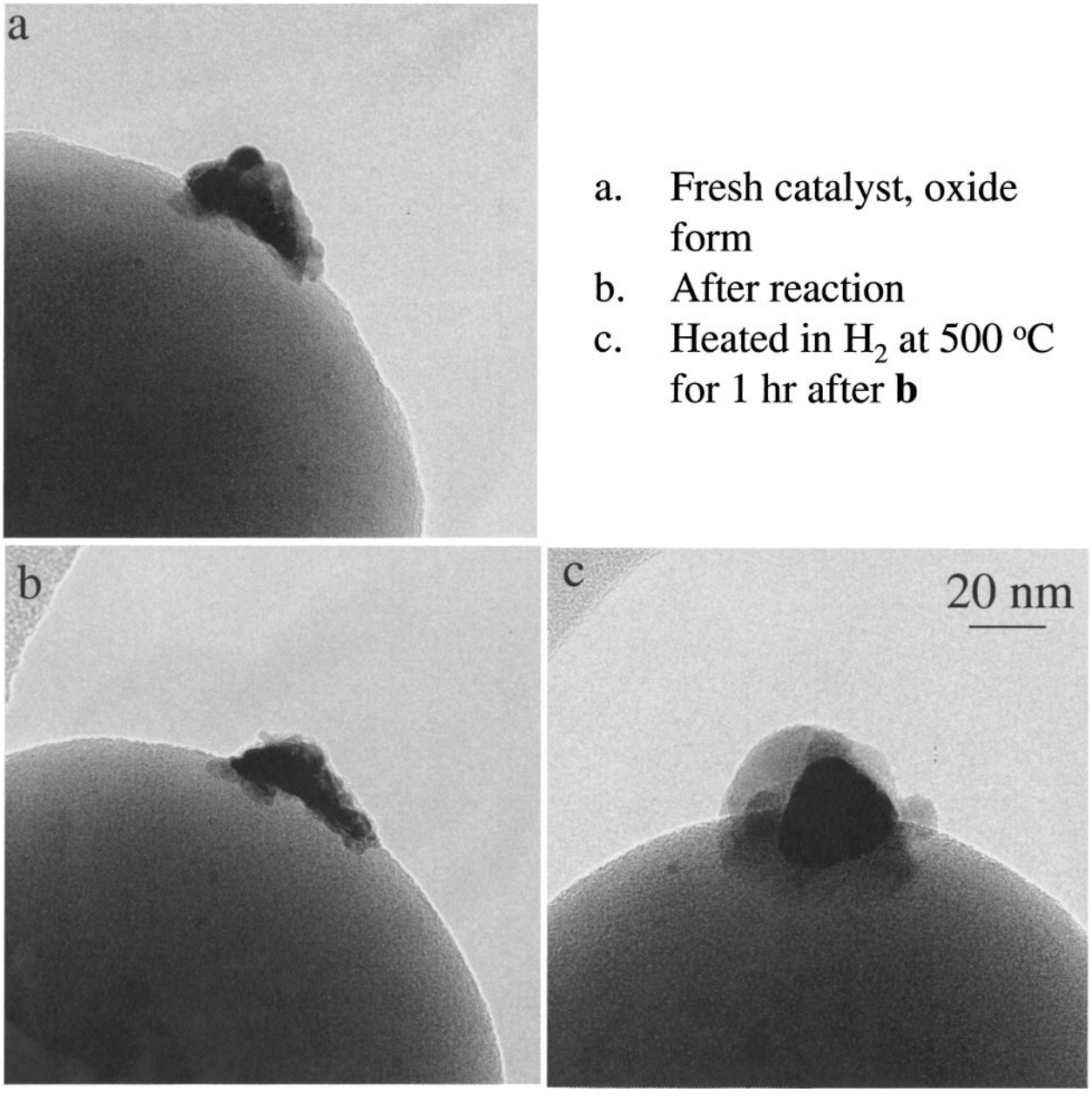

FIG. 8. Higher-magnification view of the sample as it is activated *in situ* and further reduced in H_2 at 500°C. Lattice fringes corresponding to PdO are seen in (a). The particle shrinks in size due to reduction in (b). Higher-temperature reduction makes the metal particles more spherical, but leaves a lighter contrast residue, which represents carbonaceous deposits on the metal surface.

A study of Pd–Ag catalyst particles was reported by Phillips *et al.* (18) in the context of butadiene hydrogenation. These authors found that oxidation caused a phase segregation into PdO and silver oxide (at low temperatures <200°C) and metallic Ag (at higher temperatures ~400°C). When reduced under reaction conditions, a Pd–Ag alloy did not form at all. Reduction in H_2 at higher temperatures (~400°C) was necessary for alloy formation. The evidence for alloy formation came from X-ray diffraction, which could be used because of the higher metal loading in their work, as well as the larger metal particle sizes. While XRD may provide evidence for bulk alloy formation, surface alloy formation can be directly studied only by techniques that provide the requisite spatial resolution, such as scanning probe microscopy. The STM study of the Ag/Pt system by Roder *et al.* (19) is relevant to the phenomena we have observed in our work and is described in more detail below.

The Ag/Pt system studied by Roder *et al.* (19) shares some common features with the Ag/Pd system we have studied in

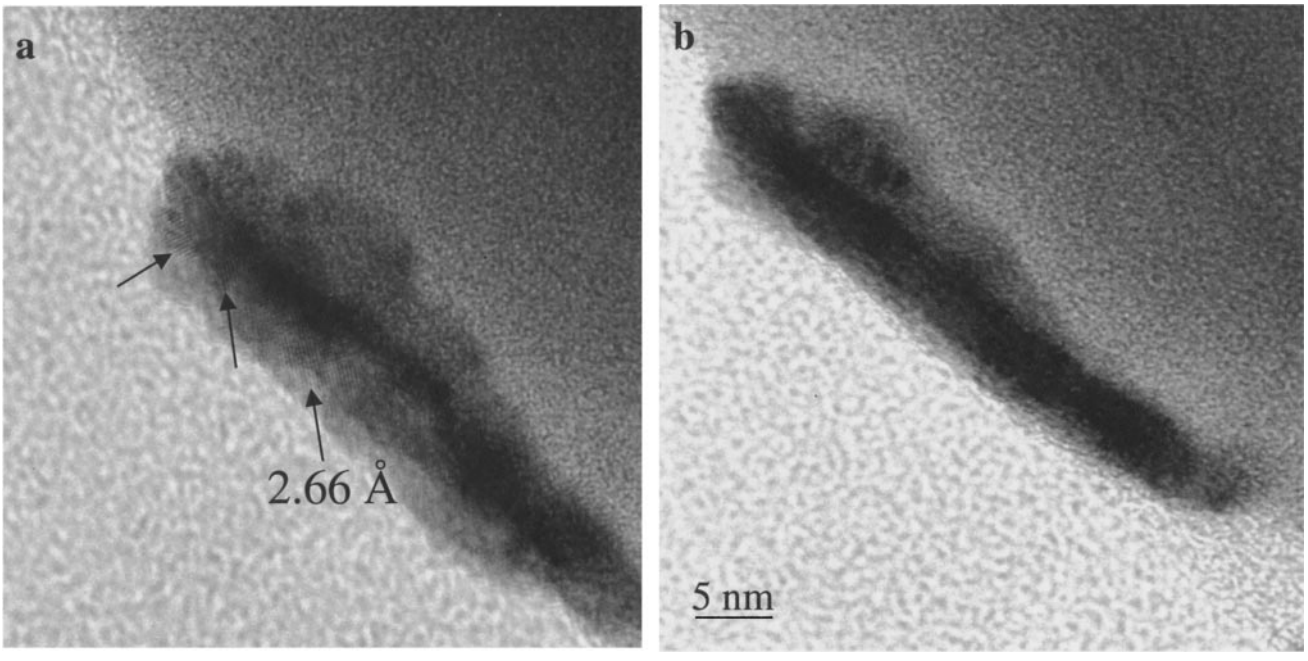

FIG. 9. Higher-magnification view of the Pd–Ag particles in their oxidized state (a) and after activation *in situ* under reaction conditions (b). The reduced form of the catalyst does not show any lattice fringes.

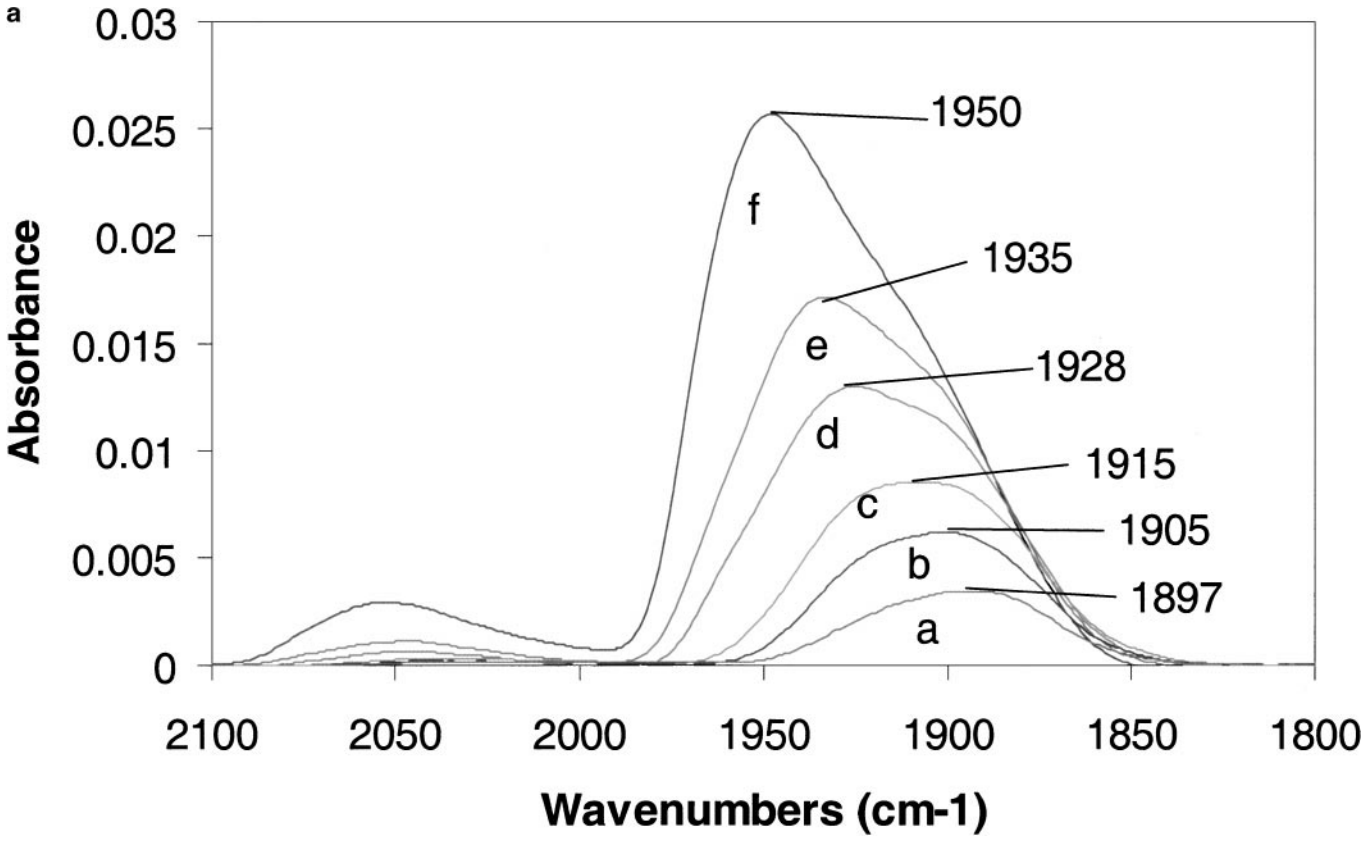

FIG. 10. IR difference spectra before and after CO addition for Pd/Silica catalyst reduced at (a) 70°C and (b) 400°C: (a) 1 pulse, (b) 2 pulses, (c) 3 pulses, (d) 10 pulses, (e) 5 min 101 ppm CO, (f) 1 min 190 Torr CO. The catalyst was preconditioned under a C_2H_2/H_2 reaction mixture for 10 min at 50°C prior to CO adsorption.

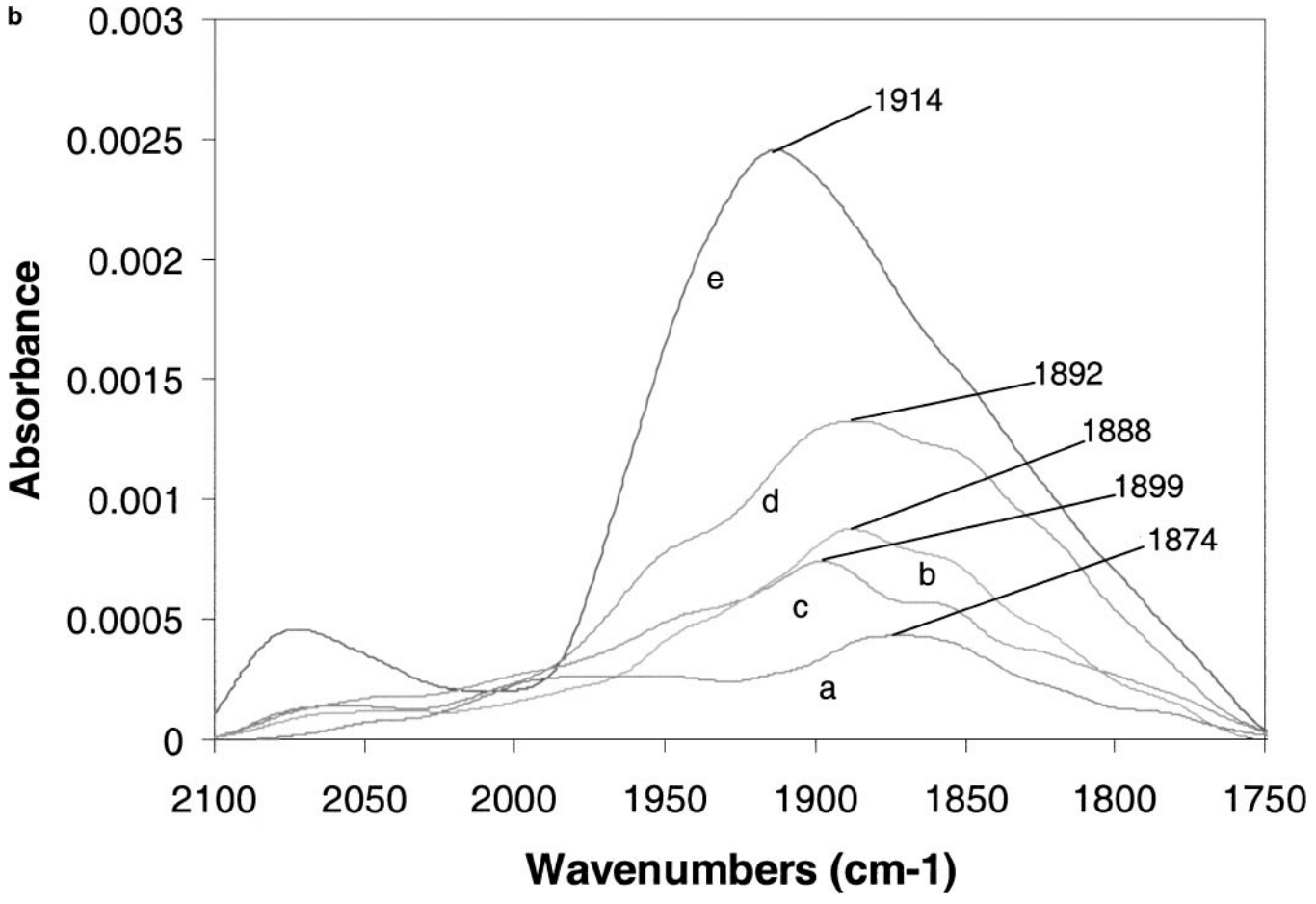

FIG. 10—*Continued*

our work. The energetics determining surface segregation of the adsorbed Ag atoms are similar for both these systems. According to theoretical calculations by Christiansen *et al.* (20), the Ag atoms should stay at the surface in segregated form, rather than forming an alloy. This is exactly what was found by Roder *et al.* (19) for Ag/Pt. At low temperatures, Ag formed a pseudomorphic surface layer, yielding large islands of Ag on the Pt(111) surface. After heating to elevated temperatures, the Ag diffused to form smaller islands only a few Ångstroms in diameter within the Pt layer. The Ag was confined to the surface, and did not diffuse into the bulk of the Pt crystal even after heating to 900 K, where the Ag eventually desorbed. At low surface concentrations of Ag, they found small Ag islands of about 10 Å in size dispersed in the Pt. At higher surface concentrations of Ag, small Pt islands of similar size were found dispersed within the Ag layer. We suspect that similar changes could be occurring in our Ag/Pd bimetallic particles as they are heated at higher-temperatures. The higher-temperature treatment in H_2 could enhance the mobility of surface Ag atoms, leading to surface structures where domains of Pd are separated by islands of Ag. These structure changes are shown schematically in Fig. 12.

The high-temperature treatment of the Pd–Ag catalysts has two beneficial effects. First, the production of oligomers is suppressed (Fig. 4), leading to improved selectivity. Second, the nonselective hydrogenation of ethylene is also suppressed as temperature is raised above the cleanup temperature (Fig. 3). Both these beneficial effects could result from the altered surface arrangement of Ag adatoms on the Pd surface. The oligomerization reaction requires multiple C_2H_2 molecules, which would not be present if the Pd sites are surrounded by Ag adatoms. Likewise, the Ag adatoms might lower the concentration of H_2 in the vicinity of the catalyst sites, allowing the ethylene to desorb instead of becoming further hydrogenated. To facilitate such structural changes, it would be beneficial to have a support that does not bind the Ag too strongly, allowing the Ag atoms to move around more easily. The silica support we have employed is quite unique, since it consists of nonporous particles with a convex curvature and a surface that is extensively hydroxylated due to its method of preparation. Our future work is directed at investigating fully the role of the support in facilitating structural rearrangements that lead to optimal selectivity for acetylene hydrogenation.

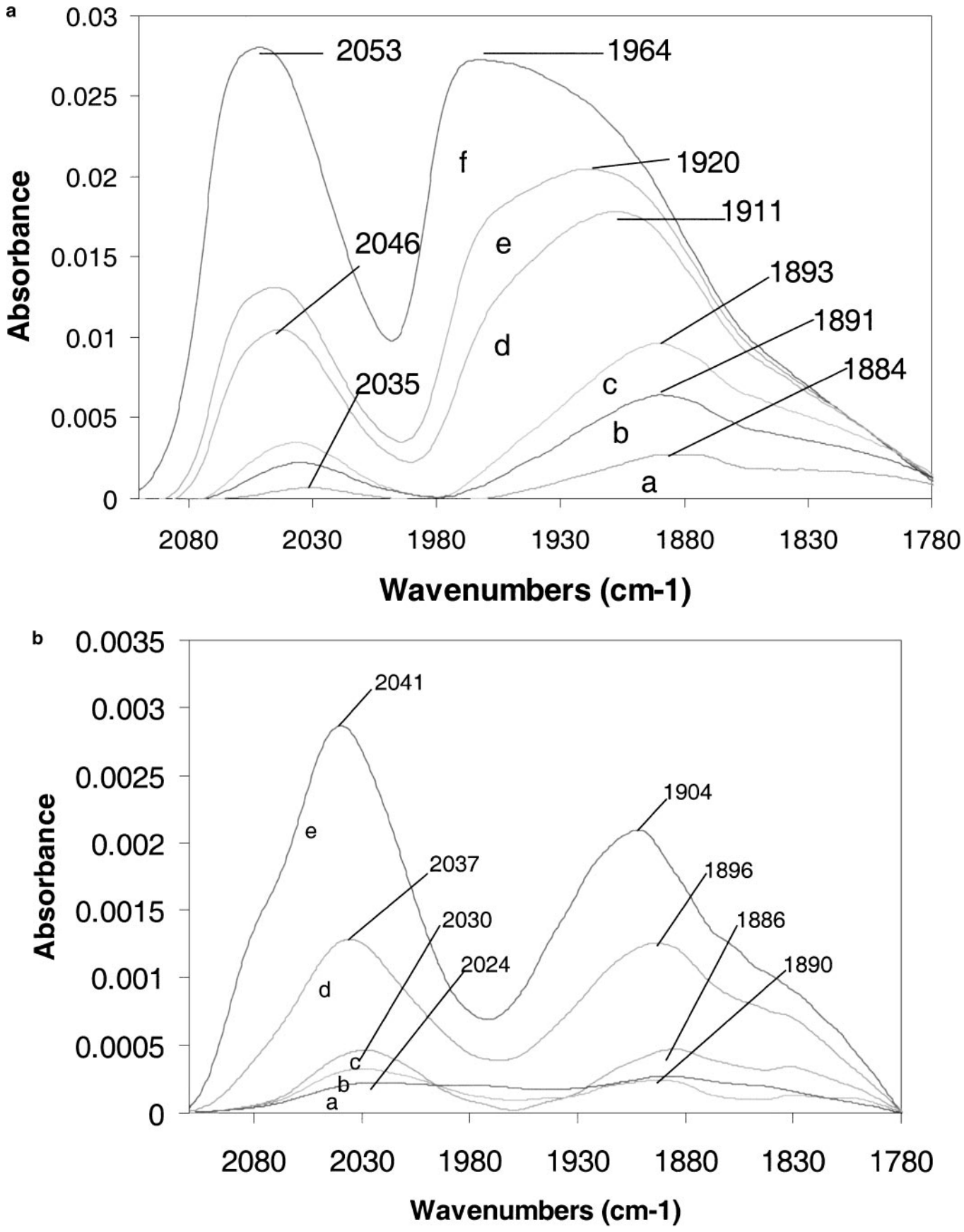

FIG. 11. IR difference spectra before and after CO addition for Pd/Ag/Silica catalyst reduced at (a) 70°C and (b) 400°C: (a) 6 pulses, (b) 10 pulses, (c) 5 s 101 ppm CO, (d) 5 min 101 ppm CO, (e) 1 min 190 Torr CO. The catalyst was preconditioned under a C_2H_2/H_2 reaction mixture for 10 min at 50°C prior to CO adsorption.

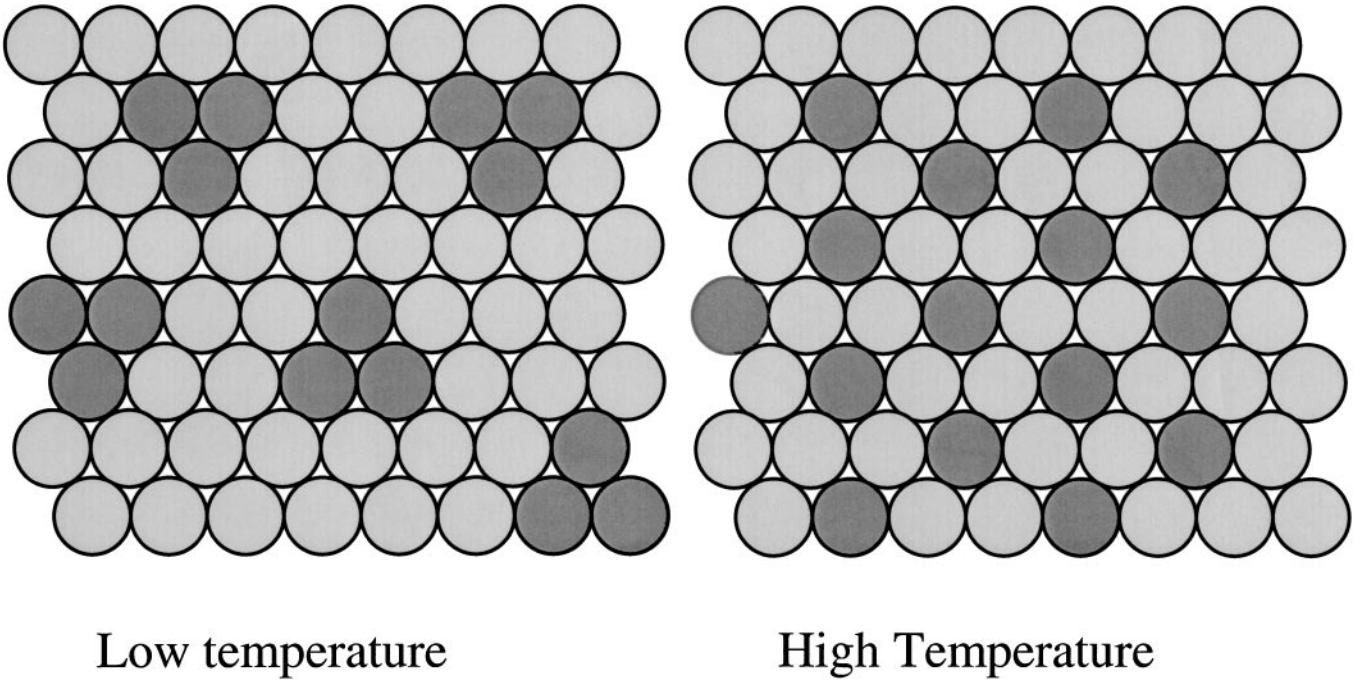

FIG. 12. Schematic diagram showing the effect of reduction temperature on the surface of Pd–Ag catalysts.

CONCLUSIONS

Oxidation of Pd and Pd–Ag catalysts transforms metallic particles into the oxide form, leading to an increase in volume and the formation of rough, irregular particle shapes. Low-temperature reduction in H_2 or *in situ* reduction in the reaction mixture transforms the particles into metallic form, but the particle shapes remain irregular. Further treatment at higher temperatures ($>400^\circ$C) is necessary to change the shape of the metal particles to spherical, faceted metal particles. The changes in morphology, by themselves, do not appear to influence the selectivity of acetylene hydrogenation to ethylene. However, when Ag is present with the Pd, the higher-temperature reduction dramatically improves the reaction selectivity and suppresses the formation of oligomeric by-products. At higher-temperatures, the Ag is mobile and is able to better distribute over the Pd surface. IR spectra of adsorbed CO show that the presence of Ag affects the bonding of CO, favoring linear CO over the bridged forms. The effect is even more pronounced after higher-temperature reduction in H_2. We propose that the effect is geometric in nature, a dilution of Pd sites by Ag that leads to a suppression of the bridged form of CO over the linear form. These results have profound implications for the operation of Pd–Ag catalysts. A catalyst that has been subjected to an oxidative regeneration cycle to burn off accumulated hydrocarbon residues shows the lowest selectivity. Catalyst restructuring during high-temperature H_2 pretreatments appears to be beneficial to obtaining the best performance from these catalysts.

ACKNOWLEDGMENTS

We acknowledge support for this work from the Department of Energy, Office of Science, via Grant DE-FG03-98ER14917, PAIR (Partnership for Academic Industrial Research). This research was supported, in part, by the Dow Chemical Company. Electron microscopy was performed at the University of New Mexico (UNM) electron microscopy facility, supported by the National Science Foundation and by the Department of Earth and Planetary Sciences at UNM.

REFERENCES

1. Than, N. C., Diillion, B., Sarrazin, P., and Cameron, C., "Catalytic Hydrogenation Process and a Catalyst for Use in the Process," U.S. Patent 5,889,187 (1999).
2. Sarkany, A., Weiss, A. H., and Guczi, L., *J. Catal.* **98**, 550 (1986).
3. Gigola, C. E., Aduriz, H. R., and Bodnariuk, P., *App. Catal.* **27**, 133 (1986).
4. Bond, G. C., Dowden, D. A., and Mackenzie, N., *Faraday Soc. Trans.* **54**, 1537 (1958).
5. Frevel, L. K., and Kressley, L. J., "Selective Hydrogenation of Acetylene in Ethylene and Catalyst Therefor," U.S. Patent 2802889 (1957).
6. Johnson, M. M., Walker, D. W., and Nowack, G. P., "Selective Hydrogenation Catalyst," U.S. Patent 4,404,124 (1983).
7. Cosyns, J., and Durand, D., "Process for Selectively Hydrogenating a Di-olefin in a Mixture of Hydrocarbons Having at Least 4 Carbon Atoms and Comprising an Alpha-Olefin," U.S. Patent 4409410 (1983).
8. Aduriz, H. R., Bodnariuk, P., Garcia, M. A., and Gigola, C. E., "Characterization, Activity and Selectivity of Palladium/Alumina in the Hydrogenation of Acetylene," Actas Simp. Iberoam. Catal., 9th, 1, 787 (1984).
9. Duca, D., Frusteri, F., Parmaliana, A., and Deganello, G., *Appl. Catal. A* **146**, 269 (1996).
10. Shin, E. W., Choi, C. H., Chang, K. S., Na, Y. H., and Moon, S. H., *Catal. Today* **44**, 137 (1998).

11. King, S. T., *Appl. Spectrosc.* **34**, 632 (1980).
12. Lambert, C. K., and Gonzalez, R. D., *Catal. Lett.* **57**, 1 (1999).
13. Zhang, Q. W., Li, J., Liu, X. X., and Zhu, Q. M., *Appl. Catal. A* **197**, 221 (2000).
14. Huang, D. C., Chang, K. H., Pong, W. F., Tseng, P. K., Hung, K. J., and Huang, W. F., *Catal. Lett.* **53**, 155 (1998).
15. Ignatova, K., Nikolova, L., and Dimov, W., *J. Phys. Chem. B* **101**, 6891 (1997).
16. Wang, S. F., Huebner, W., and Huang, C. Y., *J. Am. Ceram. Soc.* **75**, 2232 (1992).
17. Basualto, J., Barcelo, C., and Gaete, A., *Rev. Metal.* **32**, 314 (1996).
18. Phillips, J., Auroux, A., Bergeret, G., Massardier, J., and Renouprez, A., *J. Phys. Chem.* **97**, 3565 (1993).
19. Roder, H., Schuster, R., Brune, H., and Kern, K., *Phys. Rev. Lett.* **71**, 2086 (1993).
20. Christensen, A., Ruban, A. V., Stoltze, P., Jacobsen, K. W., Skriver, H. L., Norskov, J. K., and Besenbacher, F., *Phys. Rev. B* **56**, 5822 (1997).